MEF2D haploinsufficiency downregulates the NRF2 pathway and renders photoreceptors susceptible to light-induced oxidative stress

Saumya Nagar[a], Sarah M. Noveral[a,b,c], Dorit Trudler[a,b], Kevin M. Lopez[a,b], Scott R. McKercher[a,b], Xuemei Han[d], John R. Yates III[d], Juan C. Piña-Crespo[a], Nobuki Nakanishi[a,b], Takumi Satoh[a,b,e], Shu-ichi Okamoto[a,b,1], and Stuart A. Lipton[a,b,c,d,2]

[a]Neuroscience and Aging Research Center and Graduate School of Biomedical Sciences, Sanford Burnham Prebys Medical Discovery Institute, La Jolla, CA 92037; [b]Neurodegenerative Disease Center, Scintillon Institute, San Diego, CA 92121; [c]Department of Neurosciences and Program in Biomedical Sciences, School of Medicine, University of California, San Diego, La Jolla, CA 92093; [d]Department of Molecular Medicine, The Scripps Research Institute, La Jolla, CA 92037; and [e]Department of Anti-Aging Food Research, School of Bioscience and Biotechnology, Tokyo University of Technology, Tokyo 192-0982, Japan

Edited by Constance L. Cepko, Harvard Medical School/Howard Hughes Medical Institute, Boston, MA, and approved March 22, 2017 (received for review August 8, 2016)

Gaining mechanistic insight into interaction between causative factors of complex multifactorial diseases involving photoreceptor damage might aid in devising effective therapies. Oxidative stress is one of the potential unifying mechanisms for interplay between genetic and environmental factors that contribute to photoreceptor pathology. Interestingly, the transcription factor myocyte enhancer factor 2d (MEF2D) is known to be important in photoreceptor survival, as knockout of this transcription factor results in loss of photoreceptors in mice. Here, using a mild light-induced retinal degeneration model, we show that the diminished MEF2D transcriptional activity in *Mef2d*$^{+/-}$ retina is further reduced under photostimulation-induced oxidative stress. Reactive oxygen species cause an aberrant redox modification on MEF2D, consequently inhibiting transcription of its downstream target, nuclear factor (erythroid-derived 2)-like 2 (NRF2). NRF2 is a master regulator of phase II antiinflammatory and antioxidant gene expression. In the *Mef2d* heterozygous mouse retina, NRF2 is not up-regulated to a normal degree in the face of light-induced oxidative stress, contributing to accelerated photoreceptor cell death. Furthermore, to combat this injury, we found that activation of the endogenous NRF2 pathway using proelectrophilic drugs rescues photoreceptors from photo-induced oxidative stress and may therefore represent a viable treatment for oxidative stress-induced photoreceptor degeneration, which is thought to contribute to some forms of retinitis pigmentosa and age-related macular degeneration.

MEF2D | AMD | LIRD | NRF2 | proelectrophilic drug

Blindness due to photoreceptor loss from a number of diseases is a prevalent and devastating condition in the human population. Genetic predisposition and environmental stress play major roles in the incidence and progression of the retinal degeneration. Understanding disease mechanisms and interactions of causative factors should help in the design of treatment strategies. Recent evidence indicates that oxidative stress, contributing to photoreceptor cell death, plays a significant role in the pathophysiology of nonsyndromic retinitis pigmentosa (RP) and possibly age-related macular degeneration (AMD) (1–3). Moreover, light-induced oxidative stress is known to potentiate photoreceptor loss in genetic models mimicking a number of human retinal degenerations (4–11).

The oxidizing microenvironment of the retinal pigment epithelium (RPE)–photoreceptor complex has been predominantly attributed to high oxygen demand, abundant polyunsaturated fatty acids, and direct exposure to light, coupled with the adjacent choroidal hemodynamics (12). Light exposure compounded over many years in the presence of photosensitizers may prime photoreceptors and RPE for free radical/oxidative damage (12–14). In some animal models of photoreceptor degeneration, including RP and Leber congenital amaurosis, disease progression is accelerated by exposure to light and slowed by rearing in darkness (3, 15). Advanced age also compromises the endogenous antioxidant capacity of cells, increasing the amount of reactive oxygen species (ROS) (16, 17). Thus, even though heterogeneous risk factors have been implicated in photoreceptor degeneration, it is possible that they result in a final common pathway of oxidative stress.

A complex interaction between genetic susceptibility and environmental influences governs the onset and severity of photoreceptor disease (18, 19). Identifying the mechanism(s) linking these risk factors might help early detection of disease and should aid in future design of efficient and early therapeutic interventions. In the present study, to begin to determine how environmental risk factors might trigger disease onset in genetically susceptible individuals, we studied the interaction between light-induced oxidative stress and genetic mutation in myocyte enhancer factor 2d (*Mef2d*)$^{+/-}$ mice. The transcription factor MEF2D is known to influence photoreceptor survival; complete knockout results in massive photoreceptor degeneration in mouse models, and a number of humans are known to be *Mef2*

Significance

Currently, there is no effective treatment for blindness resulting from loss of photoreceptors in humans. Elucidating degenerative pathways in photoreceptors may thus facilitate therapeutic strategies. Myocyte enhancer factor 2d (MEF2D) is a transcription factor known to be important for photoreceptor survival. Here, we explore the impact of low-level environmental light exposure on photoreceptor loss in *Mef2d*-haploinsufficient mice. We elucidate a mechanism linking genes and environment, implicating oxidative stress in photoreceptor pathology. Specifically, we identify the MEF2D–nuclear factor (erythroid-derived 2)-like 2 (NRF2) pathway as a therapeutic target for photoreceptor survival. The transcription factor NRF2 stimulates antioxidant and antiinflammatory cascades. We find that activation of NRF2 with the pro-electrophilic drug carnosic acid can protect *Mef2d*-haploinsufficient photoreceptors from light-induced damage.

Author contributions: S.N., J.C.P.-C., T.S., S.-i.O., and S.A.L. designed research; S.N., K.M.L., X.H., and J.C.P.-C. performed research; S.N., J.R.Y., N.N., S.-i.O., and S.A.L. analyzed data; and S.N., S.M.N., D.T., S.R.M., J.C.P.-C., N.N., and S.A.L. wrote the paper.

Conflict of interest statement: The Sanford-Burnham Medical Research Institute (now called Sanford Burnham Prebys Medical Discovery Institute) filed a patent application for cytoprotection by congeners of carnosic acid with S.A.L. and T.S. as joint inventors.

This article is a PNAS Direct Submission.

[1]Present address: Takeda Pharmaceutical Company, Ltd., Tokyo 103-8668, Japan.

[2]To whom correspondence should be addressed. Email: slipton@ucsd.edu.

This article contains supporting information online at www.pnas.org/lookup/suppl/doi:10.1073/pnas.1613067114/-/DCSupplemental.

haploinsufficient, potentially representing a risk factor for photoreceptor disease (20–22). For this purpose, we used a variant of the rodent light-induced retinal degeneration (LIRD) model to simulate light as an environmental insult (23–26). In our model, brief environmentally relevant levels of light exposure result in photoreceptor degeneration, which allows investigation of the sequential degeneration events at the molecular and cellular level.

Here, we characterize the degenerative process that occurs in *Mef2d*$^{+/-}$ photoreceptors in this modified LIRD model that uses moderate light exposure, which does not induce photoreceptor damage in wild-type (WT) mice. Mechanistically, we show that excessive ROS in this LIRD model leads to decreased MEF2 activity via a posttranslational modification of MEF2 at cysteine 39 (causing a sulfonation adduct). The presence of this adduct interferes with the ability of the transcription factor to bind to DNA (27, 28), thus preventing activation of its downstream targets. We show that heterozygosity for *Mef2d* partially decreases MEF2D transcriptional activity, rendering photoreceptors more susceptible to an oxidizing light insult. Genetic mutation of one *Mef2d* allele coupled with environmentally induced inhibition of the activity of the second allele's normal gene product via oxidative posttranslational modification results in photoreceptor degeneration. This "double-hit" hypothesis for photoreceptor loss could also account for onset later in life as light damage accumulates; thus, this model may be relevant in some respects to AMD or secondary loss of cones in RP. Furthermore, we show that oxidation of MEF2 leads to deficient activation of the nuclear factor (erythroid-derived 2)-like 2 (NRF2, also known as *Nfe2L2*) antioxidant and antiinflammatory transcriptional pathway. This deficit in NRF2 activity impairs the cell's ability to fight photooxidative insult. To combat this light-induced oxidative stress, we treat the *Mef2d*$^{+/-}$ mouse exposed to LIRD with the novel proelectrophilic compound carnosic acid (CA) (29). Proelectrophilic compounds enhance the endogenous antioxidant capacity of retinal cells during light damage (30). We show that this antioxidant ability prevents sulfonation of MEF2D and hence inhibition of its activity, thus preserving photoreceptor function. Therefore, in this context the MEF2D–NRF2 pathway represents a potential drug target for photoreceptor degeneration, and one that is amenable to treatment with CA.

Results

***Mef2d* Wild-Type and Heterozygous Retinas Are Morphologically Indistinguishable.** Recent studies (20, 21) have demonstrated the presence of age-dependent photoreceptor degeneration in *Mef2d*$^{-/-}$ (knockout) mice, consistent with an antiapoptotic function of MEF2 in the retina, as demonstrated previously in other tissues (31). To assess if reduction in MEF2 activity contributes to photoreceptor cell death, we used *Mef2d* heterozygous mice to partially decrease MEF2D activity and determine whether photoreceptor degeneration is exacerbated in *Mef2d*$^{+/-}$ mice when exposed to oxidative stress/light damage. As expected, *Mef2d*$^{+/-}$ mice express half the amount of protein compared with *Mef2d*$^{+/+}$ (WT) mice (Fig. 1 *A* and *B*). We initially examined whether *Mef2d*$^{+/-}$ retinas also undergo photoreceptor degeneration. At developmental stage postnatal day (P) 10, P60, and P180, *Mef2d*$^{+/+}$ and *Mef2d*$^{+/-}$ retina appeared similar in hematoxylin and eosin (H&E)-stained sections (Fig. S1 *A–D*). We then performed a terminal deoxynucleotidyl transferase dUTP nick end labeling (TUNEL) assay at P14, after retinal development is complete, to rule out possible apoptotic cell death. Quantification of TUNEL-positive cells in the optic nerve head region revealed no significant difference in *Mef2d*$^{+/+}$ and *Mef2d*$^{+/-}$ mice (Fig. S1 *E* and *F*). Correspondingly, microelectroretinogram (microERG) recordings at P60 showed no functional impairment with regard to photoreceptor light responses (Fig. S1*G*). These findings indicate that *Mef2d*$^{+/-}$ photoreceptors, unlike their null (*Mef2d*$^{-/-}$) counterparts, do not undergo degeneration in an age-dependent manner and are morphologically and functionally similar to *Mef2d*$^{+/+}$ retina.

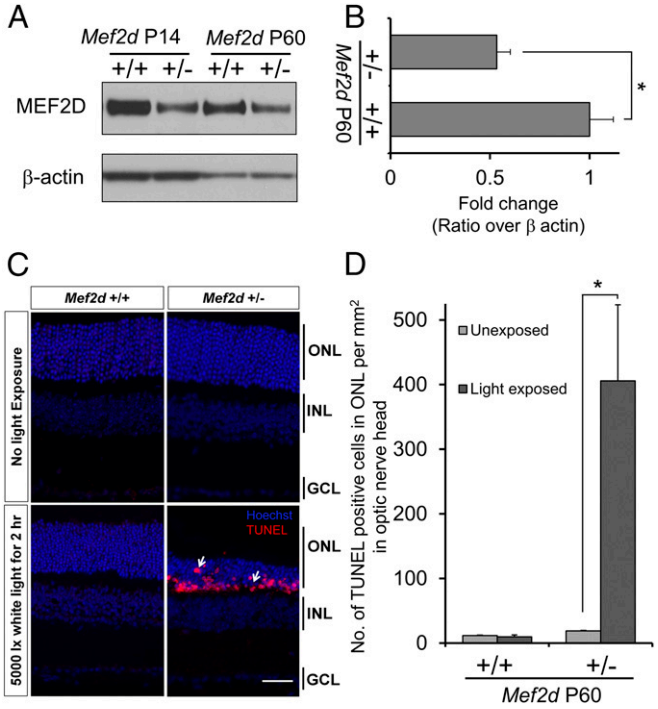

Fig. 1. *Mef2d* heterozygosity renders photoreceptors more susceptible to light damage. (*A*) Western blot analysis of MEF2D expression in *Mef2d*$^{+/+}$ and *Mef2d*$^{+/-}$ mice. (*B*) Densitometric analysis of MEF2 immunoblots ($n = 4$). (*C*) Representative micrographs of TUNEL-stained cells (red, indicated by arrows) in retinal sections in *Mef2d*$^{+/+}$ and *Mef2d*$^{+/-}$ mice. (*D*) Graph showing total number of TUNEL-positive cells per square millimeter of ONL in the optic nerve head region. Values are mean + SEM ($n = 4$, $^*P < 0.02$ by two-tailed Student's *t* test).

***Mef2d*$^{+/-}$ Retina Are Susceptible to Light-Induced Stress.** Having found no evidence for photoreceptor degeneration in *Mef2d*$^{+/-}$ mice (Fig. S1), we next asked if *Mef2d* heterozygosity might render photoreceptors more susceptible to environmental stress conditions such as oxidative insult. Generation of ROS has been associated with photoreceptor degeneration, as observed in the dry form of AMD, and has been shown to occur in response to excessive light (30, 32). We exposed dark-adapted P45-60 *Mef2d*$^{+/+}$ control (WT) mice and *Mef2d*$^{+/-}$ mice to 5,000 lux (lx) of white light for 2 h in a light box, followed by 7 d under dark conditions. Then, we determined the extent of light-induced damage using TUNEL staining on retinal sections. After light exposure, *Mef2d*$^{+/-}$ retinas showed an increased number of TUNEL-positive and shrunken photoreceptor cells in the outer nuclear layer (ONL), reflecting apoptotic cell death, compared with light-exposed *Mef2d*$^{+/+}$ control retinas (Fig. 1 *C* and *D*). This result indicates that *Mef2d*$^{+/-}$ mice are more susceptible to phototoxicity than their WT littermates in our mouse model of LIRD.

Light-Induced Reactive Oxygen Species Disrupt MEF2 Activity. Increased ROS generation is a hallmark of light-induced retinal degeneration (26). We used the fluorescent indicator MitoSOX to monitor ROS production by mitochondria in photoreceptors after light exposure. We observed elevated levels of MitoSOX fluorescence in *Mef2d*$^{+/-}$ mice within 30 min of photostimulation at 5,000 lx (Fig. 2 *A* and *B*). We and others have shown that excessive ROS production can result in posttranslational modification of protein cysteine thiols, leading to alterations in functional activity (33, 34). To determine if these levels of ROS can oxidize MEF2D in a similar manner, we used DCP-Bio1 to probe for sulfenated (-SOH) MEF2D adducts in intact retinas

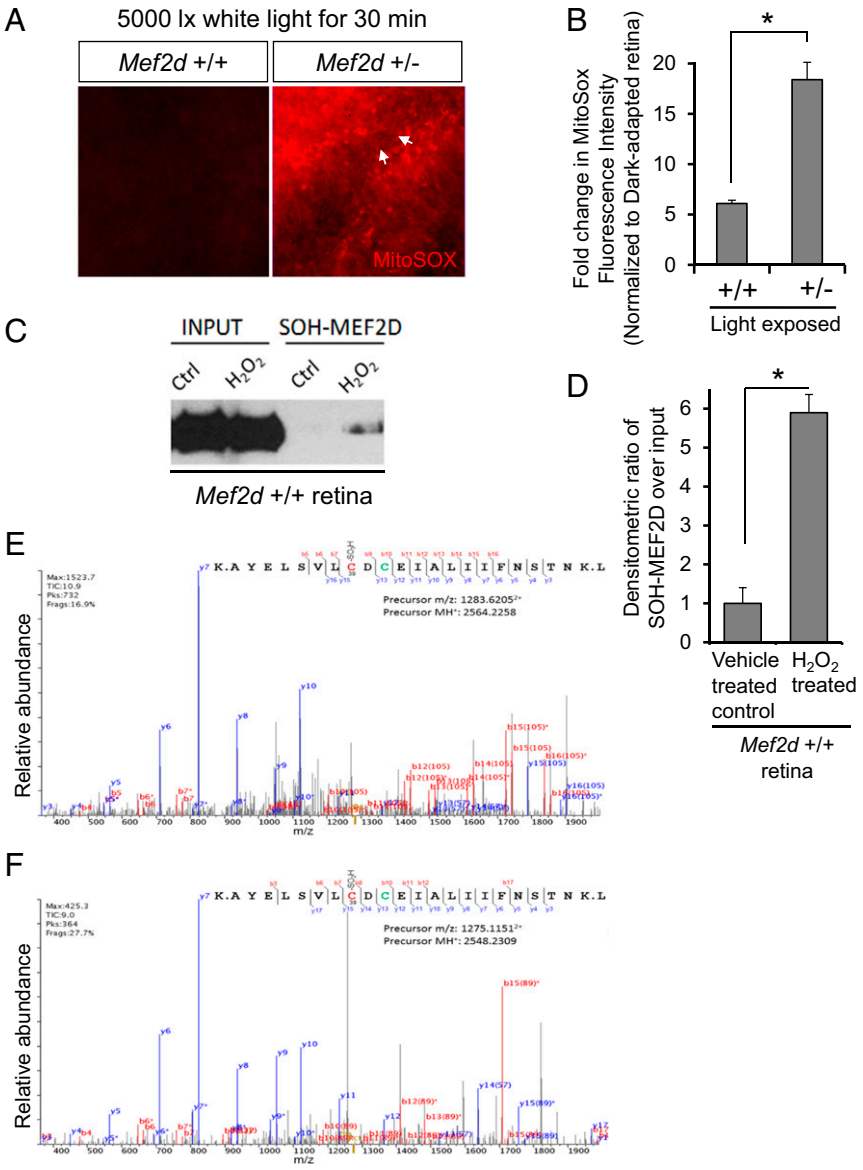

Fig. 2. ROS aberrantly modify MEF2 protein. (*A*) Representative MitoSOX imaging of photoreceptors (arrows) in light-exposed *Mef2d*$^{+/+}$ and *Mef2d*$^{+/-}$ retinas (imaged at the photoreceptor focal plane). (*B*) Quantification of MitoSOX fluorescence. Values are mean + SEM ($n = 4$, $^*P < 0.0005$ by Student's *t* test). (*C*) Detection of SOH-MEF2D in WT retinas after exposure to 500 μM H_2O_2 using DCP-Bio1 as an alkylating sulfenic acid probe and subsequent immunoblot with anti-MEF2D antibody. (*D*) Densitometry of immunoblots. Values are mean + SEM ($n = 3$, $^*P < 0.002$). (*E* and *F*) Liquid chromatography (LC)-MS/MS spectra showing SO_3H (*E*) and SO_2H (*F*) adduct formation on MEF2 at Cys39. The unoxidized Cys41 residue was labeled with iodoacetamide (+57 Da, in green). Collision-induced dissociation (CID)-mediated fragmentation of MEF2 peptide resulted in formation of "b" and "y" ion series corresponding to the N-terminal (red) and C-terminal (blue) fragments, respectively.

exposed to hydrogen peroxide as a ROS generator. Using immunoblots, we detected increased SOH-MEF2D in retinas exposed to 500 μM H_2O_2 relative to control (Fig. 2 *C* and *D*). To determine if MEF2 can be further oxidized to higher oxidation states (i.e., $SO_{2/3}H$ derivatives), we performed mass spectrometry (MS) on recombinant MEF2 following H_2O_2 exposure. We detected both sulfonated (-SO_3H) and sulfinated (-SO_2H) adducts of cysteine (Cys) 39, indicated by a 47.9847-Da and a 31.9898-Da mass shift, respectively (Fig. 2 *E* and *F*). Our group has previously shown—via reporter gene assays, chromatin immunoprecipitation (ChIP), and electrophoretic mobility shift assay—that post-translational redox modification of Cys39 inhibits MEF2 transcriptional activity by interfering with DNA binding (27, 28, 35, 36). Hence, it might be expected that excessive ROS exposure would lead to the formation of SO_XH-MEF2D ($x = 1$–3), thereby impairing transcription of MEF2 target genes.

MEF2D Modulates NRF2 Activity. To begin to test the premise that transcriptional targets of MEF2 might be aberrantly disrupted in photostimulated retinas, we initially performed pathway analysis of our published microarray data from human embryonic stem cell-derived neural/photoreceptor precursor cells expressing a constitutively active form of MEF2 (MEF2CA) to identify potentially relevant MEF2 targets (37). In particular, we assessed MEF2 transcriptional targets that would be expected to be up-regulated during oxidative stress, as occurs in photoreceptor degeneration with light damage, and found that the NRF2 antioxidant/antiinflammatory pathway represented one such target. In line with this finding, retinas from *Nrf2* knockout mice have been shown to exhibit AMD-like phenotypes

(38). Moreover, NRF2 overexpression is known to be protective in genetic models of photoreceptor degeneration (39).

To determine if MEF2D drives NRF2 expression in the proper context, we analyzed *Mef2d*$^{-/-}$ retinas at P12, before the beginning of photoreceptor cell death. We monitored *Nrf2* gene expression by qPCR and NRF2 protein levels by Western blot and observed a 70% decrease in NRF2 mRNA levels and a 50% decrease in NRF2 protein in *Mef2d*$^{-/-}$ retina (Fig. 3). To investigate MEF2D binding to the *Nrf2* promoter, we performed ChIP on P12 *Mef2d*$^{+/+}$ and *Mef2d*$^{-/-}$ retinas. We found a more than twofold increase in MEF2 binding to the *Nrf2* promoter in *Mef2d*$^{+/+}$ compared with *Mef2d*$^{-/-}$ (Fig. 4*A*). These results are consistent with the notion that MEF2D is involved in *Nrf2* transcriptional activation.

Because oxidation of MEF2 at its critical cysteine (Cys39) hinders its ability to bind to DNA, we analyzed MEF2 binding to the *Nrf2* promoter after oxidative stress. To mimic ROS-induced MEF2 oxidation in LIRD, we treated *Mef2d*$^{+/+}$ retina with 500 μM H_2O_2 for 1 h ex vivo and then performed ChIP analysis. MEF2 oxidation attenuated its binding to the *Nrf2* promoter by 25% (Fig. 4*B*). We then performed a luciferase reporter assay in P1 retinal explants to evaluate if MEF2 directly regulates *Nrf2* transcription. We electroporated an *Nrf2* promoter reporter construct into P1 *Mef2d*$^{+/+}$ and *Mef2d*$^{-/-}$ retinas and harvested them for luciferase assay after 4 d in culture. We observed that *Nrf2* activity was increased twofold in *Mef2d*$^{+/+}$ over *Mef2d*$^{-/-}$ retina (Fig. 4*C*).

Dysregulated NRF2 Activity in Light-Damaged *Mef2d*$^{+/-}$ Retina. Given that redox modification of MEF2 alters its transcriptional activity, we monitored NRF2 levels in light-exposed *Mef2d*$^{+/+}$ and *Mef2d*$^{+/-}$ mouse retinas. We observed an ∼40% increase in total *Nrf2* mRNA levels 3 h after light exposure in *Mef2d*$^{+/+}$ compared with dark-adapted mice; however, the levels remained unchanged in *Mef2d*$^{+/-}$ mice (Fig. 5*A*). These data are consistent with decreased transcriptional activity due to redox-modified MEF2D. Additionally, we found a 25%, statistically significant increase in NRF2 protein expression in *Mef2d*$^{+/+}$ retina compared with *Mef2d*$^{+/-}$ after light exposure (Fig. 5 *B* and *C*). Consistent with this, we observed a significant decrease in the up-regulation of downstream phase II genes controlled by NRF2 in *Mef2d*$^{+/-}$ retina after light exposure compared with *Mef2d*$^{+/+}$ retina (Fig. 5*D*). Taken together, these results are consistent with the notion that oxidation of Cys39 on MEF2 prevents full activation of NRF2 transcription and its downstream targets in light-exposed mouse retina. This effect is exacerbated in *Mef2d*$^{+/-}$ mice, as they have diminished MEF2 protein activity compared with *Mef2d*$^{+/+}$ that is further inactivated in the presence of ROS.

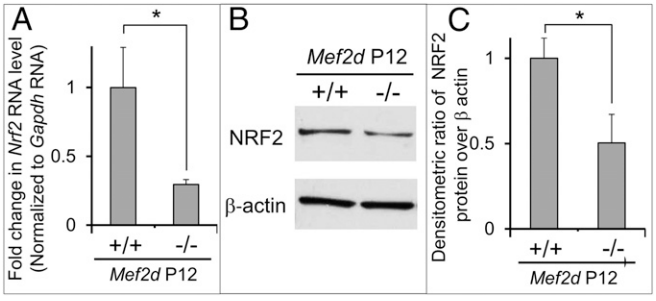

Fig. 3. Altered NRF2 expression in *Mef2d*$^{-/-}$ retina. (*A*) qPCR analysis of *Nrf2* mRNA in *Mef2d*$^{-/-}$ P12 retina relative to *Mef2d*$^{+/+}$. Values are mean + SEM (n = 6, *P < 0.04 by Student's t test). (*B*) Immunoblot analysis of NRF2 protein levels in *Mef2d*$^{-/-}$ retina at P12. (*C*) Densitometry of immunoblots. Values are mean + SEM (n = 3, *P < 0.04).

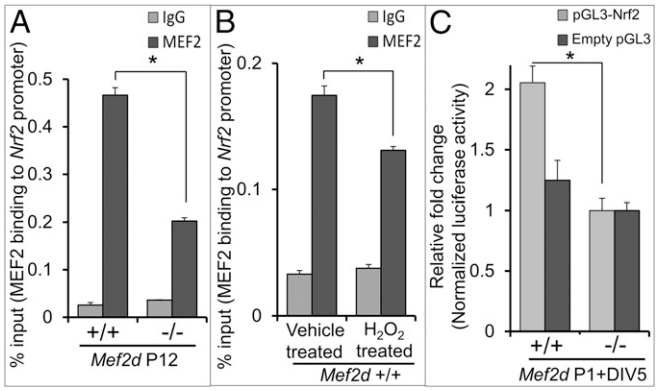

Fig. 4. MEF2D binds to and activates the *Nrf2* promoter. (*A*) ChIP analysis of P12 *Mef2d*$^{+/+}$ and *Mef2d*$^{-/-}$ retina. Values are mean + SEM (n = 4, *P < 0.00002 by Student's t test). Residual MEF2 signal was observed in *Mef2d*$^{-/-}$ retina because the antibody also recognizes other MEF2 isoforms. (*B*) ChIP analysis of *Mef2d*$^{+/+}$ retina after exposure to H_2O_2. Values are mean + SEM (n = 4, *P < 0.003 by Student's t test). (*C*) Quantification of *Nrf2* promoter reporter activity in P1 *Mef2d*$^{+/+}$ and *Mef2d*$^{-/-}$ retinal explants. Explants were coelectroporated with *Nrf2* promoter-driven firefly luciferase construct and internal Renilla luciferase control. Values are mean + SEM (n = 6, *P < 0.02 by Student's t test). DIV, days in vitro.

Carnosic Acid Confers Neuroprotection in Vivo to Light-Exposed *Mef2d*$^{+/-}$ Retinas. Because we found evidence for ROS generation and impaired NRF2 up-regulation in *Mef2d*$^{+/-}$ retinas exposed to light, we next sought to combat the increased ROS by up-regulating the endogenous NRF2 pathway. We have previously shown that CA, a proelectrophilic compound found in the herb rosemary, readily crosses the blood–retina barrier and protects WT photoreceptors in albino rats from prolonged light-induced retinal degeneration related to oxidative stress (30). We showed that CA up-regulates endogenous antioxidant phase II enzymes via the NRF2 transcriptional pathway. Moreover, this pathway is largely responsible for the mechanism of CA action because silencing *Nrf2* significantly abrogated the protective effect (30, 40–43). Here, we wanted to determine if CA could provide neuroprotection in the *Mef2d*$^{+/-}$ mice model of LIRD (44).

We have previously shown that CA induces NRF2 translocation to the nucleus where it binds to the antioxidant response element (ARE) consensus sequence in the promoter region of phase II genes, including glutamyl cysteine ligase modifier subunit (*Gclm*), glutamyl cysteine ligase catalytic subunit (*Gclc*), hemeoxygenase-1 (*Hmox1*, encoding HO-1), NADPH quinone oxidoreductase 1(*Nqo1*), ATP-dependent reductase, sulfiredoxin 1 (*Srxn1*), Na^+-independent cystine-glutamate exchanger (*Slc7a11*, encoding xCT), and superoxide dismutase (*Sod1/2/3*) (45, 46). Induction of these endogenous antiinflammatory and antioxidant genes is cytoprotective. To validate these findings in our *Mef2d*$^{+/-}$ mouse model of LIRD, we performed RT-qPCR and immunoblotting experiments 3 h after light exposure. We observed that treatment with CA up-regulated RNA and protein expression of ARE-dependent genes in light-exposed *Mef2d*$^{+/-}$ mice (Fig. 6*A*). To ascertain if CA-induced antioxidant pathways detoxify ROS generated in *Mef2d*$^{+/-}$ mice, we used MitoSOX to detect ROS 30 min after light exposure in *Mef2d*$^{+/-}$ mice with or without CA pretreatment. CA-treated retinas showed significantly decreased MitoSOX fluorescence compared with untreated light-exposed retina (Fig. 6*B*).

Next, we asked if treatment with CA could protect photoreceptors from light-induced cell death. We quantified the total number of TUNEL-positive cells in CA- and vehicle-treated retinal sections 7 d after light exposure. We found that CA treatment significantly decreased the number of apoptotic

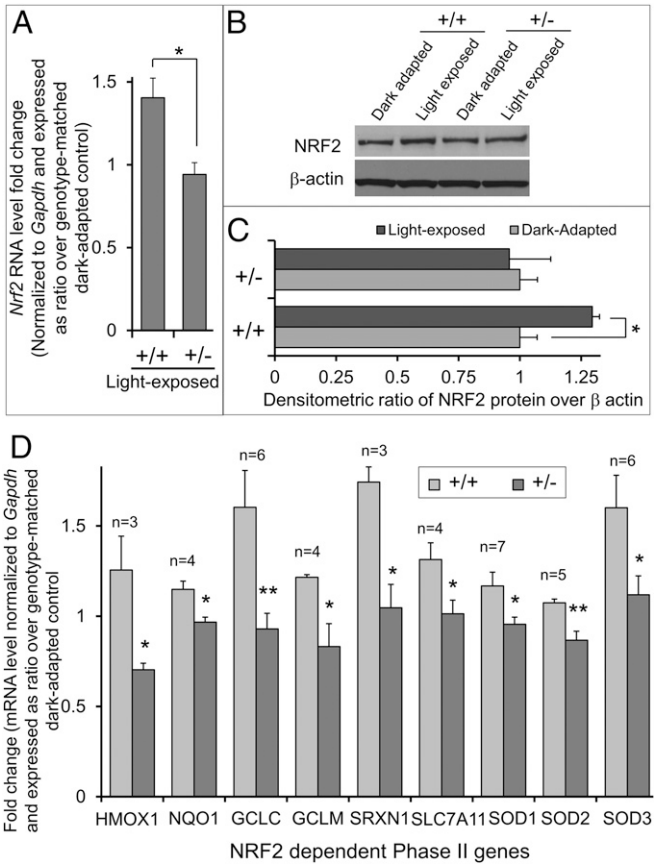

Fig. 5. Impaired up-regulation of NRF2 after light damage in *Mef2d*$^{+/-}$ mice. (*A*) qPCR shows *Nrf2* mRNA expression in light-exposed *Mef2d*$^{+/+}$ and *Mef2d*$^{+/-}$ mouse retina. Levels in light-exposed retinas were normalized to genotype-matched dark-adapted control retinas. Values are mean + SEM ($n = 5$, $^*P < 0.02$ by Student's *t* test). (*B*) NRF2 immunoblot in light-exposed *Mef2d*$^{+/+}$ and *Mef2d*$^{+/-}$ mice. (*C*) Quantification of immunoblots by densitometric analysis. Values are mean + SEM ($n = 4$, $^*P < 0.05$ by two-way ANOVA). (*D*) mRNA levels of NRF2 downstream genes in light-exposed *Mef2d*$^{+/+}$ compared with *Mef2d*$^{+/-}$ retinas. Values are mean + SEM ($^*P < 0.05$, $^{**}P < 0.01$ by Student's *t* test).

photoreceptor cells in *Mef2d*$^{+/-}$ retina compared with vehicle (Fig. 7 *A* and *B*). Furthermore, there was no significant difference between control untreated/unexposed retina and CA-treated/light-exposed retina. Consistent with these findings, we observed a similar ONL thickness under these conditions (Fig. 7*A*).

Additionally, to determine whether CA treatment can preserve photoreceptor function in the face of potentially damaging light exposure, we recorded microERGs to test photoreceptor light responsiveness using a multielectrode array (MEA). In a normal electroretinogram (ERG), the initial a-wave represents the photoreceptor light response, and the ensuing b-wave originates from second-order retinal neurons, including bipolar cells. With MEA recordings, we monitored ex vivo the light responses of photoreceptors in isolated retinas at various regions of interest. Because damage to the superior retina is the most severe in our LIRD model, we positioned superior retinal photoreceptors directly in contact with the electrodes of the MEA to record localized light-elicited responses. Our ERG assessment confirmed that CA treatment preserved photoreceptor function after light exposure. The a- and b-wave amplitudes were significantly greater in light-exposed CA-treated mice compared with vehicle-treated (Fig. 7 *C* and *D*). Taken together, our results show that CA conferred both histological and functional protection to photoreceptors.

Discussion

In the present study, we develop a mouse model to investigate the mechanism whereby the interaction of genes and environment (GxE) can contribute to photoreceptor degeneration. Specifically, ambient light exposure is shown to induce oxidative stress that consequently impairs MEF2D transcriptional activity via oxidation of a critical cysteine residue (Cys39) near the DNA-binding domain. Subsequently, this aberrant posttranslational modification leads to dysregulation of NRF2 signaling and hence to inadequate activation of downstream antioxidant pathways, which contributes to photoreceptor cell death. We also provide evidence for a potential therapeutic approach aimed at boosting the endogenous NRF2 antioxidant pathway using the proelectrophilic compound CA.

Considering the possible etiologies of photoreceptor degeneration, genetic predisposition, multiple environmental risk factors, and their complicated interactions make it difficult to devise a therapeutic strategy to target each risk factor separately (18, 26, 47, 48). One risk factor, oxidative stress, has been implicated as an important mechanism contributing to cell death in several neurodegenerative diseases, including photoreceptor loss in the dry form of AMD and nonsyndromic RP (2, 13, 49, 50). Oxidative stress may cause damage to proteins, nucleic acids, and lipids, rendering it a potentially important therapeutic target (1, 3, 15). As demonstrated here and elsewhere, light exposure can result in the generation of excessive ROS. This fact, coupled with the sensitivity of RPE and photoreceptors to oxidative stress, makes the photoreceptor degeneration observed in the *Mef2d* heterozygous retina upon exposure to moderate light levels a

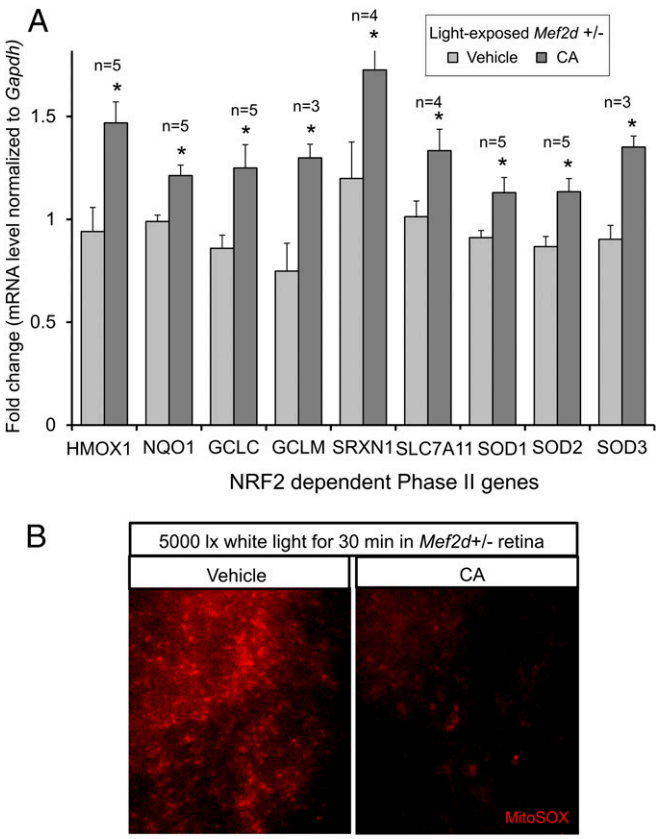

Fig. 6. CA decreases ROS in light-exposed *Mef2d*$^{+/-}$ retina. (*A*) RT-qPCR of ARE-dependent phase II genes in light-exposed *Mef2d*$^{+/-}$ retina following CA treatment. Values are mean + SEM. (*B*) Superoxide production detected by MitoSOX Red in light-exposed *Mef2d*$^{+/-}$ mice after CA treatment.

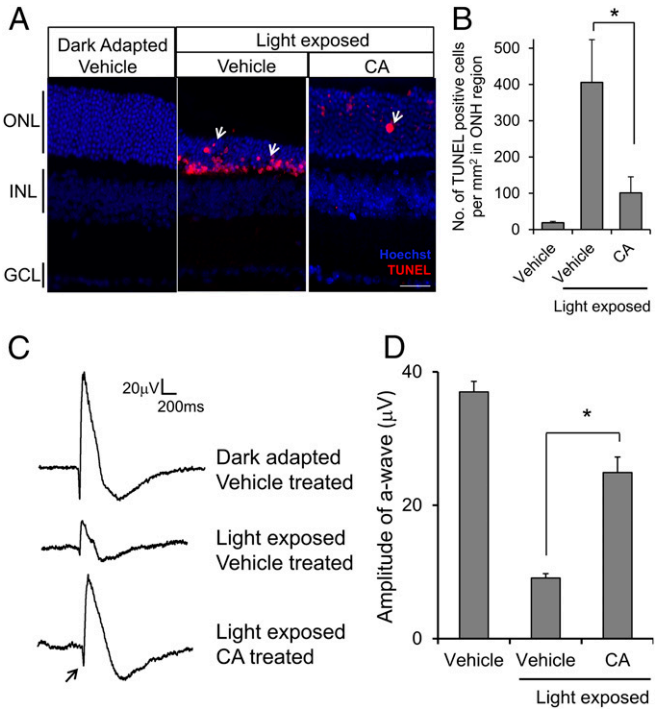

Fig. 7. CA treatment protects *Mef2d*$^{+/-}$ photoreceptors from light damage. (*A*) Representative images of TUNEL-stained photoreceptors (red; arrows) in retinal sections in light-exposed *Mef2d*$^{+/-}$ mice after CA treatment. (*B*) Quantification of TUNEL-positive cells in ONL of *Mef2d*$^{+/-}$ with or without CA treatment. Values are mean + SEM ($n = 4$, $^*P < 0.05$ by Student's *t* test). (*C*) Representative ERG traces showing light responses in *Mef2d*$^{+/-}$ with or without CA treatment. Arrow indicates a-wave. (*D*) Quantification of a-wave amplitude after CA treatment in light-damaged *Mef2d*$^{+/-}$ retina. Values are mean + SEM ($n = 3$, $^*P < 0.0.0001$ by Student's *t* test).

tractable model to evaluate GxE interactions. We used 5,000 lx of light, which represents a much less intense stimulus than encountered in bright sunlight at midday (10,000–25,000 lx) (26). Therefore, our model is pathophysiologically relevant in terms of human light exposure. We show that exposure of mice to this relatively low level of light is sufficient to induce ROS production and consequent oxidative stress within 30 min of light exposure in pigmented mice heterozygous for the *Mef2d* gene but not in WT littermate mice. This finding is a strong indication that the adverse effects that we observed after exposure to this low level of light reflects increased vulnerability in our animal model due to lack of one copy of *Mef2d*. One week following a 2-h light exposure, retinas isolated from *Mef2d*$^{+/-}$ mice exhibited significantly increased photoreceptor cell death compared with WT littermate controls. These results are consistent with the notion that photoreceptors haploinsufficient for *Mef2d* are unable to combat oxidative stress.

We next provide evidence that ROS generated due to light exposure causes a specific oxidation reaction on MEF2D, contributing to cell death in part because of inhibition of its anti-apoptotic transcriptional activity. Previously, our group and others have shown that aberrant thiol oxidation (protein sulfonation or *S*-nitrosylation) is implicated in multiple neurodegenerative disorders, contributing to disease etiology and progression (34, 51). Oxidation of proteins in general has been reported in retinal degeneration (3, 12, 14, 52). Thus, oxidative stress is thought to cause progressive adduct formation, inhibiting protein function (53). Also, nitration of tyrosine residues on proteins, e.g., forming nitrotyrosine, is known to mediate some forms of oxidative stress (13). Here, we demonstrate a direct reaction between ROS species and MEF2D protein that inhibits MEF2D transcriptional activity. *Mef2d* heterozygosity also impairs this activity. Light-induced ROS generation leads to sulfenic (-SOH), sulfinic (-SO_2H), and sulfonic (-SO_3H) acid adduct formation on the gene product of the remaining *Mef2d* allele, preventing MEF2 transcriptional activation of NRF2. With compromised NRF2 signaling, inadequate antioxidant phase II enzymes are induced, resulting in increased vulnerability of photoreceptors in the *Mef2d*$^{+/-}$ retina to light exposure.

NRF2 orchestrates the regulation of cellular antioxidant and antiinflammatory defense responses (54–56). Oxidative stress results in release of NRF2 from its cytoplasmic-binding partner KELCH-like ECH-associated protein 1 (KEAP1), allowing translocation of NRF2 into the nucleus, where it activates transcription by binding to antioxidant response elements in the regulatory regions of phase II genes, including *Hmox1*, *Nqo1*, *Gclm*, *Slc7a11*, *Srxn1*, and *Sod1/2/3* (55, 56). NRF2 signaling has been proposed as a therapeutic candidate for photoreceptor degeneration, neurodegenerative disorders, diabetes, cancer, and cardiovascular diseases because it provides extensive cellular protection via activation of multiple genes (57–60). In fact, BG-12 (dimethyl fumarate) was recently approved by the Food and Drug Administration as an NRF2 activator to treat the relapsing/remitting form of multiple sclerosis (61, 62). Supporting a role for NRF2 in photoreceptor degeneration, published evidence shows that *Nrf2* knockout and *Sod2* knockdown in animal models produces an AMD-like phenotype (38, 63).

Importantly, we report a therapeutic strategy to bolster endogenous NRF2 signaling in light-exposed *Mef2d*$^{+/-}$retinas using the proelectrophilic drug CA (1, 37, 50, 51). CA is a natural product found in herbs such as rosemary and sage. Antioxidant therapy has been used in dry AMD with limited success, in part because traditional antioxidant treatment necessitates frequent and high dosage to achieve and sustain sufficient systemic drug levels that must also be able to cross the blood–retina barrier (29, 64, 65). However, such treatment lacks target specificity and often cannot reach the proper target. As an alternative approach, NRF2 activation by electrophilic compounds has been attempted but often exerts adverse side effects. For example, many electrophilic compounds, including sulforaphane, curcumin, and dimethyl fumarate, react with the major thiol in cells, glutathione (GSH), thereby compromising endogenous antioxidant activity in healthy cells (29). In contrast, we previously discovered that proelectrophilic drugs (PEDs) become active electrophiles capable of reaction with thiol-containing proteins only after exposure to oxidative stress, as occurs in photoreceptors of light-exposed *Mef2d*$^{+/-}$ mice. Because in these cells undergoing oxidative stress GSH has already been depleted, upon conversion to the active electrophile PEDs such as CA are free to react with an active thiol group on KEAP1, thus releasing NRF2 to enter the nucleus. Moreover, unlike electrophilic compounds, PEDs do not deplete GSH from healthy cells because in the absence of oxidative stress PEDs are not converted to their active electrophilic form (1, 37, 50, 51, 66). Our group previously used CA to protect WT albino rats from severe light-induced photoreceptor damage (30). Here, we used transnasal administration of CA to protect photoreceptors from much lower levels of light exposure that would otherwise induce oxidative stress and photoreceptor cell death in *Mef2d*$^{+/-}$ mice. We have previously shown that CA readily crosses the blood–brain and blood–retina barriers, conferring neuroprotection via activation of NRF2-regulated phase II genes (30, 41). Because CA enhances the endogenous antioxidant defense mechanism specifically at the site of injury, it may also prove effective in counteracting other diseases in which oxidative stress has been implicated in the pathogenic mechanism.

The results of our study support the "multiple-hit" model of photoreceptor degeneration, implicating interaction of the gene

(in this case *Mef2d*) and an environmental factor (here, light exposure); hence, such GxE interactions may affect an individual's risk for the disease (15, 18). We show that *Mef2d* heterozygosity alters cellular responses to stress but does not manifest a retinal phenotype by itself until triggered by the environmental susceptibility factor. Finally, we show that we can overcome even complex GxE interactions that result in photoreceptor degeneration by augmenting the endogenous antioxidant capacity using a PED approach to provide long-term, safe, and targeted therapy.

Materials and Methods

Mice. *Mef2d*$^{+/+}$, *Mef2d*$^{+/-}$, and *Mef2d*$^{-/-}$ mice were bred on a mixed 129Sv/C57BL6 background (67) and kept under a 12-h light/12-h dark cycle. All procedures were performed according to institutional and NIH-approved Guidelines for Animal Research and the Association for Research in Vision and Ophthalmology statement on the Use of Animals.

LIRD. Littermate adult WT control mice and *Mef2d*$^{+/-}$ mice, age P45–P60, were dark-adapted for 24 h. Pupils were dilated with atropine sulfate eye drops before a 2-h exposure to 5,000 lx of diffuse, cool, white fluorescent light in a light box made of clear plastic. After light exposure, the mice were kept in total darkness for 7 d before histological assessment and for 3 h before RNA analysis. Note that the Met450 variant of the gene encoding a retinal pigment epithelium-specific 65-kDa protein (RPE65), which is found in C57BL6J, renders the photoreceptors of these mice resistant to light damage. In contrast, the Leu450 variant of RPE65, as found in 129Sv, increases their sensitivity to light (68, 69). We therefore genotyped mice in our colony by DNA sequencing and found only the Leu variant at the *Rpe65* locus in both the *Mef2d*$^{+/+}$ (WT) and *Mef2d*$^{+/-}$ (het) mice. Hence, our results cannot be explained away due to differences in RPE65 variants between the WT and het *Mef2d* mice.

ONL Thickness Measurement. Mice were euthanized by isoflurane overdose and enucleated with the superior region of the eye marked with animal tattoo ink on the cornea (Ketchum Manufacturing). Eyes were fixed with 4% paraformaldehyde (PFA) and embedded in paraffin. Sections 5 μm in thickness were cut through the optic disk of each eyeball, stained with H&E, and imaged with ImageScope software (Aperio). ONL thickness was measured in the inferior and superior hemispheres at 200-μm intervals starting at the optic nerve head. Mean values from the left and right eye for each mouse were calculated.

TUNEL Assay. To view apoptotic photoreceptors, we performed TUNEL assays using the In Situ Cell Death Detection Kit (Roche) according to the manufacturer's instructions. Images were acquired in the inferior and superior regions on both sides of the optic nerve head. The total number of TUNEL-positive cells in the ONL per field-of-view were counted, and the ratio of TUNEL-positive cells to total cells in the ONL region was calculated.

Immunoblot Detection of Sulfenated MEF2D. This protocol was modified from published procedures (70, 71) to capture oxidized retinal proteins. Adult retinas were exposed to 500 μM H_2O_2 and then treated with 100 μM DCP-Bio1 (KeraFAST), a biotinylated cysteine sulfenic acid (R-SOH) probe, in serum-free medium (DMEM/F12, 100 U/mL penicillin, 100 μg/mL streptomycin, 0.29 mg/mL L-glutamine, 5 μg/mL insulin) for 1 h at 37 °C. Retinas were washed in PBS and homogenized in lysis buffer formulated to diminish protein oxidation upon exposure to atmospheric oxygen. To prepare lysis buffer, 100 μM diethylenetriamine pentaacetic acid, 10 mM *N*-ethylmaleimide, 10 mM iodoacetamide, and protease inhibitor mixture (Thermo Scientific) were dissolved in T-PER Tissue Protein Extraction Reagent (Thermo Scientific). Protein lysates were then applied to Zeba desalting columns (Thermo Scientific) to remove excess DCP-Bio1. After quantifying total protein content using a bicinchoninic acid (BCA) assay kit (Thermo Scientific), 750 μg of total lysate in 2 M urea was incubated with High Capacity Streptavidin Agarose (Thermo Scientific) overnight at 4 °C to capture DCPBio1-tagged proteins. Beads were then washed sequentially with 1% SDS, 4 M urea in PBS, 1 M NaCl, 100 μM ammonium bicarbonate, and distilled H_2O for 5 min each. Affinity captured proteins were eluted with SDS/PAGE loading buffer, subjected to immunoblot analysis along with input samples, and detected using MEF2D antibody (1:2,000, BD Biosciences).

ERGs. Mice were dark-adapted overnight and killed by isoflurane overdose. Eyes were enucleated, and orientation was marked using animal tattoo ink. Retinas were dissected under dim red light (Wratten #2 filter) in oxygenated Ames' media (Sigma, A1420) with sodium bicarbonate buffer ($NaHCO_3$) at 34 °C. Each retina with the carrier membrane was flattened and mounted on a filter membrane with a 2-mm hole in the center and then placed in a multielectrode array (MEA; array of 60 electrodes; area: 1.96 mm^2) chamber with the ganglion cell layer against the electrodes. For LIRD recordings, the flattened retina was placed in the MEA chamber with the superior retina positioned in its center and the photoreceptor side in contact with the electrodes. The retinal tissue was held in place with a weighted mesh ring and allowed to recover in Ames' media superfused at a flow rate of 20 mL/min for 20 min. Light responses to a 200-ms stimulus were elicited using a Uniblitz shutter (Vincent Associates) attached to the microscope light source and driven by a computer-controlled stimulus generator (STG2004, Multi-Channel Systems). With the ganglion cell layer down, a negative initial current response was obtained, and with the photoreceptor side down, the wave polarity was reversed. In the case of light-damaged retinas, the photoreceptors were placed in contact with the electrodes in a fashion that facilitated recording of localized responses from areas of maximum damage in the superior retina. Traces from each electrode were extracted and converted into axon binary file format (.ABF) using MC Data Tool software (Multi Channel Systems) and analyzed using pClamp10 software (Molecular Devices). Traces were filtered at 300–500 Hz using a low-pass filter (Bessel, 8-pole). Response peak amplitude and duration were measured using pClamp10.

Detection of ROS with MitoSOX. The fluorescent dye, MitoSOX Red, was used to detect superoxide anions generated from mitochondria, as per the manufacturer's instructions (Invitrogen). Light-exposed retinas were extracted under dim red light in artificial cerebrospinal fluid (ACSF) and loaded with 2.5 μM MitoSOX in ACSF for 30 min at 37 °C. Retinas were then washed in fresh ACSF to remove excess dye and fixed in 4% PFA before imaging under an epifluorescence microscope. Fluorescence intensity was analyzed with SlideBook 5.5 software (Intelligent Imaging Innovations, Inc.).

Reporter Gene Assays After Electroporation. P1 retinas were extracted in serum-free medium (DMEM/F12, 100 U/mL penicillin, 100 μg/mL streptomycin, 0.29 mg/mL L-glutamine, 5 μg/mL insulin) and placed in an electroporation chamber (model BTX453 Microslide Chamber, Harvard Apparatus) with photoreceptors facing the anode to facilitate DNA transfer specifically to the photoreceptors. A pGL3-*Nrf2* promoter luciferase reporter construct (0.5 μg/μL, 1.7 kb, a kind gift from Qing Jun Meng, University of Manchester, Manchester, United Kingdom) or a control empty pGL3 luciferase reporter vector, plus Renilla luciferase control vector (0.1 μg/μL), were coelectroporated. DNA solution in PBS (80 μL) was placed in the chamber containing the retinas, and five square pulses (30 V) of 50-ms length with 950-ms intervals were applied using an electroporator (model ECM 830) (72, 73). Electroporated retinas were then transferred into serum-free media followed by 10% FBS-containing media for an additional 10-min recovery period. Retinal eyecups were then cultured with the lens side down on polycarbonate membranes at 37 °C for 4 d. Tissues were lysed in reporter lysis buffer (Promega), and lysates were subjected to luciferase reporter gene assay (Dual Glo, Promega) following the manufacturer's protocol.

Mass Spectrometry. Mass spectra from top-down analyses were acquired with an LTQ-Orbitrap-XL mass spectrometer (Thermo Scientific) with collision-induced dissociation (CID) or electron transfer dissociation using MEF2 recombinant protein in the presence or absence of 500 μM H_2O_2. Recombinant protein was dissolved in 1% acetic acid and 50% acetonitrile and injected via syringe into the mass spectrometer port at a flow rate of 3 mL/min.

RT-qPCR. Total RNA was extracted using a *mir*Vana RNA isolation kit (Ambion) according to the manufacturer's protocol. We used an EXPRESS One-Step SuperScript qRT-PCR Kit (Invitrogen) and a LightCycler 480 Instrument (Roche). All qPCR reactions were performed in triplicate and normalized to GAPDH mRNA expression. Predesigned primers were purchased from Integrated DNA Technologies (IDT).

ChIP Assay. ChIP experiments were performed using the ChIP-IT EXPRESS assay kit following the manufacturer's protocol (Active Motif). For ChIP after H_2O_2 treatment, adult retinas were extracted in serum-free medium (DMEM/F12, 100 U/mL penicillin, 100 μg/mL streptomycin, 0.29 mg/mL L-glutamine, and 5 μg/mL insulin) and exposed to 500 μM H_2O_2 for 1 h. For ChIP on P12 mouse retinas, *Mef2d*$^{+/+}$ and *Mef2d*$^{-/-}$ retinas were extracted in cold PBS. Tissues were cut into smaller pieces and cross-linked in 1% methanol-free formaldehyde for 10 min at room temperature, washed in PBS, and homogenized

in lysis buffer. Lysed cells were centrifuged to pellet the nuclei and resuspended in shearing buffer. Nuclei were sonicated with 20 pulses of 15-s duration to obtain 500–1,000 bp of sheared DNA. A 10-μL aliquot of this mixture was used for Input DNA. Equal proportions of chromatin and protein complex were incubated with anti-MEF2 antibody (Santa Cruz) or control rabbit IgG along with Protein G magnetic beads at 4 °C overnight. Beads were washed, and immunoprecipitated DNA was eluted and reverse cross-linked. ChIP DNA and input DNA were quantified using the EXPRESS SYBR GreenER qPCR kit in a LightCycler 480 (Roche). Fold enrichment was calculated using the Ct method.

Western Blotting. For protein expression analyses, retinas extracted in PBS were homogenized in T-PER Tissue Protein Extraction Reagent containing protease inhibitor mixture (Thermo Scientific). Protein concentration was determined using BCA reagent (Thermo Scientific). Equal amounts of samples were separated by gel electrophoresis and transferred to nitrocellulose/PVDF membranes. The following antibodies were used to assess and quantify protein expression: NRF2 (1:1,000, Abcam) and MEF2D (1:2,000, BD Biosciences).

Transnasal Treatment with CA. Mice were treated with CA or vehicle three times (on an alternate day schedule) before light exposure. CA (Nagase & Co., >91% purity) was dissolved in vehicle and administered by intranasal injection (10 mg/kg/injection). Vehicle consisted of 2-hydroxypropyl-β-cyclodextrin (HP-β-CD) to enhance the solubility of the CA (74) and 0.25% (wt/vol) chitosan, added to temporarily increase the permeability of the olfactory mucosa to facilitate improved drug delivery (44). Mice were kept under light anesthesia throughout the procedure with 1.5–2% isoflurane in a mixture of 70% nitrous oxide and 30% oxygen using an isoflurane vaporizer anesthesia machine specifically designed for rodents. A total of 12 μL of solution was applied dropwise (2 μL per drop) to each nostril alternately over the course of a few minutes. Vehicle-treated mice in the control group received the same volume of HP-β-CD.

Statistical Analyses. Statistical analyses were carried out in GraphPad Prism. Data are mean and SEM. Statistical significance was tested using a two-tailed Student's *t* test for pairwise comparisons or a two-way ANOVA and appropriate post hoc test for multiple comparisons.

ACKNOWLEDGMENTS. We thank Dr. Qing Ming for reagents. This work was supported in part by NIH Grants R01 NS086890, DP1 DA041722, and P01 HD29587; La Jolla Interdisciplinary Neuroscience Center Core Grant P30 NS076411; and a grant from the Arnold and Mabel Beckman Initiative for Macular Research.

1. Organisciak DT, Vaughan DK (2010) Retinal light damage: Mechanisms and protection. *Prog Retin Eye Res* 29:113–134.
2. Campochiaro PA, et al. (2015) Is there excess oxidative stress and damage in eyes of patients with retinitis pigmentosa? *Antioxid Redox Signal* 23:643–648.
3. Contín MA, Benedetto MM, Quinteros-Quintana ML, Guido ME (2016) Light pollution: The possible consequences of excessive illumination on retina. *Eye (Lond)* 30:255–263.
4. Sanyal S, Hawkins RK (1986) Development and degeneration of retina in rds mutant mice: Effects of light on the rate of degeneration in albino and pigmented homozygous and heterozygous mutant and normal mice. *Vision Res* 26:1177–1185.
5. Naash ML, et al. (1996) Light-induced acceleration of photoreceptor degeneration in transgenic mice expressing mutant rhodopsin. *Invest Ophthalmol Vis Sci* 37:775–782.
6. LaVail MM, Gorrin GM, Yasumura D, Matthes MT (1999) Increased susceptibility to constant light in nr and pcd mice with inherited retinal degenerations. *Invest Ophthalmol Vis Sci* 40:1020–1024.
7. Organisciak DT, Li M, Darrow RM, Farber DB (1999) Photoreceptor cell damage by light in young Royal College of Surgeons rats. *Curr Eye Res* 19:188–196.
8. Chen CK, et al. (1999) Abnormal photoresponses and light-induced apoptosis in rods lacking rhodopsin kinase. *Proc Natl Acad Sci USA* 96:3718–3722.
9. Chen J, Simon MI, Matthes MT, Yasumura D, LaVail MM (1999) Increased susceptibility to light damage in an arrestin knockout mouse model of Oguchi disease (stationary night blindness). *Invest Ophthalmol Vis Sci* 40:2978–2982.
10. Cideciyan AV, et al. (2005) In vivo dynamics of retinal injury and repair in the rhodopsin mutant dog model of human retinitis pigmentosa. *Proc Natl Acad Sci USA* 102:5233–5238.
11. Hartong DT, Berson EL, Dryja TP (2006) Retinitis pigmentosa. *Lancet* 368:1795–1809.
12. Yu DY, Cringle SJ (2005) Retinal degeneration and local oxygen metabolism. *Exp Eye Res* 80:745–751.
13. Jarrett SG, Boulton ME (2012) Consequences of oxidative stress in age-related macular degeneration. *Mol Aspects Med* 33:399–417.
14. Siu TL, Morley JW, Coroneo MT (2008) Toxicology of the retina: Advances in understanding the defence mechanisms and pathogenesis of drug- and light-induced retinopathy. *Clin Experiment Ophthalmol* 36:176–185.
15. Paskowitz DM, LaVail MM, Duncan JL (2006) Light and inherited retinal degeneration. *Br J Ophthalmol* 90:1060–1066.
16. Pinazo-Durán MD, et al. (2014) Oxidative stress and its downstream signaling in aging eyes. *Clin Interv Aging* 9:637–652.
17. Lin H, et al. (2011) Mitochondrial DNA damage and repair in RPE associated with aging and age-related macular degeneration. *Invest Ophthalmol Vis Sci* 52:3521–3529.
18. Swaroop A, Chew EY, Rickman CB, Abecasis GR (2009) Unraveling a multifactorial late-onset disease: From genetic susceptibility to disease mechanisms for age-related macular degeneration. *Annu Rev Genomics Hum Genet* 10:19–43.
19. Chen Y, et al. (2011) Assessing susceptibility to age-related macular degeneration with genetic markers and environmental factors. *Arch Ophthalmol* 129:344–351.
20. Andzelm MM, et al. (2015) MEF2D drives photoreceptor development through a genome-wide competition for tissue-specific enhancers. *Neuron* 86:247–263.
21. Omori Y, et al. (2015) Mef2d is essential for the maturation and integrity of retinal photoreceptor and bipolar cells. *Genes Cells* 20:408–426.
22. Paciorkowski AR, et al. (2013) MEF2C haploinsufficiency features consistent hyperkinesis, variable epilepsy, and has a role in dorsal and ventral neuronal developmental pathways. *Neurogenetics* 14:99–111.
23. Hafezi F, Marti A, Munz K, Remé CE (1997) Light-induced apoptosis: Differential timing in the retina and pigment epithelium. *Exp Eye Res* 64:963–970.
24. Hafezi F, et al. (1997) The absence of c-fos prevents light-induced apoptotic cell death of photoreceptors in retinal degeneration in vivo. *Nat Med* 3:346–349.
25. Noell WK, Walker VS, Kang BS, Berman S (1966) Retinal damage by light in rats. *Invest Ophthalmol* 5:450–473.
26. Wenzel A, Grimm C, Samardzija M, Remé CE (2005) Molecular mechanisms of light-induced photoreceptor apoptosis and neuroprotection for retinal degeneration. *Prog Retin Eye Res* 24:275–306.
27. Okamoto S, et al. (2014) S-nitrosylation-mediated redox transcriptional switch modulates neurogenesis and neuronal cell death. *Cell Reports* 8:217–228.
28. Ryan SD, et al. (2013) Isogenic human iPSC Parkinson's model shows nitrosative stress-induced dysfunction in MEF2-PGC1α transcription. *Cell* 155:1351–1364.
29. Satoh T, Lipton SA (2007) Redox regulation of neuronal survival mediated by electrophilic compounds. *Trends Neurosci* 30:37–45.
30. Rezaie T, et al. (2012) Protective effect of carnosic acid, a pro-electrophilic compound, in models of oxidative stress and light-induced retinal degeneration. *Invest Ophthalmol Vis Sci* 53:7847–7854.
31. Okamoto S, Krainc D, Sherman K, Lipton SA (2000) Antiapoptotic role of the p38 mitogen-activated protein kinase-myocyte enhancer factor 2 transcription factor pathway during neuronal differentiation. *Proc Natl Acad Sci USA* 97:7561–7566.
32. Klein BE, et al. (2014) Sunlight exposure, pigmentation, and incident age-related macular degeneration. *Invest Ophthalmol Vis Sci* 55:5855–5861.
33. Gu Z, et al. (2002) S-nitrosylation of matrix metalloproteinases: Signaling pathway to neuronal cell death. *Science* 297:1186–1190.
34. Nakamura T, et al. (2015) Aberrant protein S-nitrosylation contributes to the pathophysiology of neurodegenerative diseases. *Neurobiol Dis* 84:99–108.
35. Huang K, et al. (2000) Solution structure of the MEF2A-DNA complex: Structural basis for the modulation of DNA bending and specificity by MADS-box transcription factors. *EMBO J* 19:2615–2628.
36. Santelli E, Richmond TJ (2000) Crystal structure of MEF2A core bound to DNA at 1.5 A resolution. *J Mol Biol* 297:437–449.
37. Chan SF, et al. (2015) Transcriptional profiling of MEF2-regulated genes in human neural progenitor cells derived from embryonic stem cells. *Genom Data* 3:24–27.
38. Zhao Z, et al. (2011) Age-related retinopathy in NRF2-deficient mice. *PLoS One* 6:e19456.
39. Bocci V, Valacchi G (2015) Nrf2 activation as target to implement therapeutic treatments. *Front Chem* 3:4.
40. Satoh T, et al. (2008) Carnosic acid protects neuronal HT22 cells through activation of the antioxidant-responsive element in free carboxylic acid- and catechol hydroxyl moieties-dependent manners. *Neurosci Lett* 434:260–265.
41. Satoh T, et al. (2008) Carnosic acid, a catechol-type electrophilic compound, protects neurons both in vitro and in vivo through activation of the Keap1/Nrf2 pathway via S-alkylation of targeted cysteines on Keap1. *J Neurochem* 104:1116–1131.
42. Satoh T, et al. (2011) Dual neuroprotective pathways of a pro-electrophilic compound via HSF-1-activated heat-shock proteins and Nrf2-activated phase 2 antioxidant response enzymes. *J Neurochem* 119:569–578.
43. Satoh T, McKercher SR, Lipton SA (2013) Nrf2/ARE-mediated antioxidant actions of pro-electrophilic drugs. *Free Radic Biol Med* 65:645–657.
44. Vaka SR, Murthy SN, Repka MA, Nagy T (2011) Upregulation of endogenous neurotrophin levels in the brain by intranasal administration of carnosic acid. *J Pharm Sci* 100:3139–3145.
45. Zhang M, et al. (2013) Emerging roles of Nrf2 and phase II antioxidant enzymes in neuroprotection. *Prog Neurobiol* 100:30–47.
46. Xu C, Li CY, Kong AN (2005) Induction of phase I, II and III drug metabolism/transport by xenobiotics. *Arch Pharm Res* 28:249–268.
47. Ambati J, Fowler BJ (2012) Mechanisms of age-related macular degeneration. *Neuron* 75:26–39.
48. Veleri S, et al. (2015) Biology and therapy of inherited retinal degenerative disease: Insights from mouse models. *Dis Model Mech* 8:109–129.
49. Beatty S, Koh H, Phil M, Henson D, Boulton M (2000) The role of oxidative stress in the pathogenesis of age-related macular degeneration. *Surv Ophthalmol* 45:115–134.

50. Yildirim Z, Ucgun NI, Yildirim F (2011) The role of oxidative stress and antioxidants in the pathogenesis of age-related macular degeneration. *Clinics (Sao Paulo)* 66: 743–746.
51. Kriegenburg F, Poulsen EG, Koch A, Krüger E, Hartmann-Petersen R (2011) Redox control of the ubiquitin-proteasome system: From molecular mechanisms to functional significance. *Antioxid Redox Signal* 15:2265–2299.
52. Negre-Salvayre A, Coatrieux C, Ingueneau C, Salvayre R (2008) Advanced lipid peroxidation end products in oxidative damage to proteins. Potential role in diseases and therapeutic prospects for the inhibitors. *Br J Pharmacol* 153:6–20.
53. Stadtman ER, Levine RL (2000) Protein oxidation. *Ann N Y Acad Sci* 899:191–208.
54. Nguyen T, Nioi P, Pickett CB (2009) The Nrf2-antioxidant response element signaling pathway and its activation by oxidative stress. *J Biol Chem* 284:13291–13295.
55. Itoh K, et al. (1997) An Nrf2/small Maf heterodimer mediates the induction of phase II detoxifying enzyme genes through antioxidant response elements. *Biochem Biophys Res Commun* 236:313–322.
56. Itoh K, et al. (1999) Keap1 represses nuclear activation of antioxidant responsive elements by Nrf2 through binding to the amino-terminal Neh2 domain. *Genes Dev* 13: 76–86.
57. Jaramillo MC, Zhang DD (2013) The emerging role of the Nrf2-Keap1 signaling pathway in cancer. *Genes Dev* 27:2179–2191.
58. Joshi G, Johnson JA (2012) The Nrf2-ARE pathway: A valuable therapeutic target for the treatment of neurodegenerative diseases. *Recent Patents CNS Drug Discov* 7: 218–229.
59. Tan SM, de Haan JB (2014) Combating oxidative stress in diabetic complications with Nrf2 activators: How much is too much? *Redox Rep* 19:107–117.
60. Xiong W, MacColl Garfinkel AE, Li Y, Benowitz LI, Cepko CL (2015) NRF2 promotes neuronal survival in neurodegeneration and acute nerve damage. *J Clin Invest* 125: 1433–1445.
61. Fox RJ, et al.; CONFIRM Study Investigators (2012) Placebo-controlled phase 3 study of oral BG-12 or glatiramer in multiple sclerosis. *N Engl J Med* 367:1087–1097.
62. Gold R, et al.; DEFINE Study Investigators (2012) Placebo-controlled phase 3 study of oral BG-12 for relapsing multiple sclerosis. *N Engl J Med* 367:1098–1107.
63. Justilien V, et al. (2007) SOD2 knockdown mouse model of early AMD. *Invest Ophthalmol Vis Sci* 48:4407–4420.
64. Age-Related Eye Disease Study Research Group (2001) A randomized, placebo-controlled, clinical trial of high-dose supplementation with vitamins C and E, beta carotene, and zinc for age-related macular degeneration and vision loss: Age-Related Eye Disease Study (AREDS) Report Number 8. *Arch Ophthalmol* 119:1417–1436.
65. Age-Related Eye Disease Study Research Group (2000) Risk factors associated with age-related macular degeneration. A case-control study in the age-related eye disease study: Age-Related Eye Disease Study Report Number 3. *Ophthalmology* 107: 2224–2232.
66. Ahuja M, et al. (2016) Distinct Nrf2 signaling mechanisms of fumaric acid esters and their role in neuroprotection against 1-methyl-4-phenyl-1,2,3,6-yetrahydropyridine-induced experimental Parkinson's-like disease. *J Neurosci* 36:6332–6351.
67. Kim Y, et al. (2008) The MEF2D transcription factor mediates stress-dependent cardiac remodeling in mice. *J Clin Invest* 118:124–132.
68. Wenzel A, Reme CE, Williams TP, Hafezi F, Grimm C (2001) The Rpe65 Leu450Met variation increases retinal resistance against light-induced degeneration by slowing rhodopsin regeneration. *J Neurosci* 21:53–58.
69. Wenzel A, Grimm C, Samardzija M, Remé CE (2003) The genetic modifier Rpe65Leu (450): Effect on light damage susceptibility in c-Fos-deficient mice. *Invest Ophthalmol Vis Sci* 44:2798–2802.
70. Klomsiri C, et al. (2010) Use of dimedone-based chemical probes for sulfenic acid detection evaluation of conditions affecting probe incorporation into redox-sensitive proteins. *Methods Enzymol* 473:77–94.
71. Nelson KJ, et al. (2010) Use of dimedone-based chemical probes for sulfenic acid detection methods to visualize and identify labeled proteins. *Methods Enzymol* 473: 95–115.
72. Donovan SL, Dyer MA (2006) Preparation and square wave electroporation of retinal explant cultures. *Nat Protoc* 1:2710–2718.
73. Montana CL, Myers CA, Corbo JC (2011) Quantifying the activity of cis-regulatory elements in the mouse retina by explant electroporation. *J Vis Exp* 52:pii: 2821.
74. Carpenter TO, Gerloczy A, Pitha J (1995) Safety of parenteral hydroxypropyl beta-cyclodextrin. *J Pharm Sci* 84:222–225.